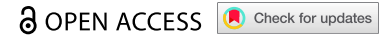


RESEARCH ARTICLE



Revisiting the truncated lamin A produced by a commonly used strain of *Lmna* knockout mice

Joonyoung R. Kim ^a, Paul H. Kim ^a, Ashley Presnell^a, Yiping Tu ^a, and Stephen G. Young ^{a,b}

^aDepartments of Medicine, David Geffen School of Medicine, University of California, Los Angeles, CA, USA; ^bDepartments of Human Genetics, David Geffen School of Medicine, University of California, Los Angeles, CA, USA

ABSTRACT

The *Lmna* knockout mouse (*Lmna*^{-/-}) created by Sullivan and coworkers in 1999 has been widely used to examine lamin A/C function. The knockout allele contains a deletion of *Lmna* intron 7–exon 11 sequences and was reported to be a null allele. Later, Jahn and coworkers discovered that the mutant allele produces a 54-kDa truncated lamin A and identified, by RT-PCR, a *Lmna* cDNA containing exon 1–7 + exon 12 sequences. Because exon 12 encodes prelamins A's CaaX motif, the mutant lamin A is assumed to be farnesylated. In the current study, we found that the truncated lamin A in *Lmna*^{-/-} mouse embryonic fibroblasts (MEFs) was predominantly nucleoplasmic rather than at the nuclear rim, leading us to hypothesize that it was not farnesylated. Our study revealed that the most abundant *Lmna* transcripts in *Lmna*^{-/-} MEFs contain exon 1–7 but not exon 12 sequences. Exon 1–7 + exon 12 transcripts were detectable by PCR but in trace amounts. We suspect that these findings explain the nucleoplasmic distribution of the truncated lamin A in *Lmna*^{-/-} MEFs, and subsequent cell transduction experiments support this suspicion. A truncated lamin A containing exon 1–7 sequence was nucleoplasmic, whereas a lamin A containing exon 1–7 + exon 12 sequences was located along the nuclear rim. Our study explains the nucleoplasmic targeting of truncated lamin A in *Lmna*^{-/-} MEFs and adds to our understanding of a commonly used strain of *Lmna*^{-/-} mice.

ARTICLE HISTORY

Received 5 July 2023
Revised 6 September 2023
Accepted 8 September 2023

KEYWORDS

Lamins; LMNA deficiency; *Lmna* transcripts; nuclear envelope; nuclear lamina; protein farnesylation


Introduction

In 1999, Sullivan *et al.* [1] reported the development of *Lmna* knockout mice (*Lmna*^{-/-}) and discovered that these mice exhibit perinatal-lethal perinatal muscular dystrophy and cardiomyopathy. To generate *Lmna*^{-/-} mice, they used a gene-targeting vector to replace a 2-kb segment of *Lmna* (from mid-intron 7 to mid-exon 11) with a *Pgkneo* cassette. Their western blotting and immunocytochemistry studies revealed that *Lmna*^{-/-} mice [and mouse embryonic fibroblasts (MEFs) from these mice] did not produce any lamin A/C protein. Later, in 2012, Jahn *et al.* [2] discovered that the ‘Sullivan knockout allele’ yields a 54-kDa truncated lamin A, and they were able to document, by RT-PCR, a 1.4-kb *Lmna* cDNA containing exon 1–7 spliced in-frame to exon 12. Because exon 12 encodes prelamins A's CaaX motif (which triggers

protein farnesylation) and because exon 11 encodes the cleavage site for ZMPSTE24 (which normally clips off the farnesylated C terminus), they assumed that the 54-kDa truncated lamin A underwent protein farnesylation and that its C-terminal farnesylcysteine methyl ester was retained and never clipped off by ZMPSTE24. This assumption seems to be supported by immunocytochemistry images of *Lmna*^{-/-} MEFs that appear to show some of the truncated lamin A at the nuclear rim.

Our group has used the ‘Sullivan *Lmna*^{-/-} mice’ extensively in studies of the nuclear lamina [3–7]. We confirm the production of the 54-kDa lamin A in *Lmna*^{-/-} MEFs. However, we were surprised to find that the truncated lamin A in *Lmna*^{-/-} MEFs is predominantly nucleoplasmic, whereas lamin B1 (a farnesylated protein) is targeted to the nuclear rim. The

CONTACT Stephen G. Young  sgyoung@mednet.ucla.edu  Departments of Medicine and Human Genetics, David Geffen School of Medicine, University of California, 675 Charles E. Young Dr. South, Los Angeles, CA 90095, USA

 Supplemental data for this article can be accessed online at <https://doi.org/10.1080/19491034.2023.2262308>

© 2023 The Author(s). Published by Informa UK Limited, trading as Taylor & Francis Group.

This is an Open Access article distributed under the terms of the Creative Commons Attribution-NonCommercial License (<http://creativecommons.org/licenses/by-nc/4.0/>), which permits unrestricted non-commercial use, distribution, and reproduction in any medium, provided the original work is properly cited. The terms on which this article has been published allow the posting of the Accepted Manuscript in a repository by the author(s) or with their consent.

observation that the truncated lamin A in *Lmna*^{-/-} MEFs was predominantly nucleoplasmic prompted us to consider the possibility that it might lack exon 12 sequences and therefore would not be farnesylated.

In the current study, we revisited the biogenesis of the truncated lamin A in *Lmna*^{-/-} MEFs [1].

Materials and methods

Cell lines

Lmna^{-/-}, *Lmna*^{-/-}*Lmnb1*^{-/-}*Lmnb2*^{-/-}, and *Zmpste24*^{-/-} MEFs have been described previously [1,3,6,8]. Immortalized mouse aortic smooth muscle cells (SMCs) (ATCC, CRL-2797) were cultured in DMEM containing 10% FBS (HyClone), 1× nonessential amino acids, 2 mM glutamine, 1 mM sodium pyruvate, and 0.2 mg/mL G418 [9].

Lmna-deficient SMCs

Lmna-deficient SMCs (*Lmna*^{-/-}) (lacking any detectable lamin A/C by western blot or by immunocytochemical staining) were created by CRISPR/Cas9 gene editing. Guide RNAs targeting *Lmna* 5' upstream sequences (5'-GGATTGGCCGCTTCTGTGCG-3') and exon 1 (5'-ATCCCCCAGCTCGGCCTCGT-3') were subcloned into the CRISPR vector pX458-GFP. A Nucleofector II apparatus (Lonza) and the Cell line T Nucleofector kit (Lonza) were used to electroporate 5 µg of each vector into 2 × 10⁶ SMCs. After 48 h, SMCs with the top 1% GFP signal intensity were sorted by flow cytometry and seeded into 96-well plates. After 10 days, genomic DNA was isolated from SMC clones with the DNeasy kit (Qiagen) and analyzed by PCR with F3 (*Lmna* 5' upstream) and R3 (*Lmna* exon 1) primers. The resulting PCR products were sequenced with F4 (*Lmna* 5' upstream sequences); DNA sequencing revealed an 888-bp deletion (412 bp of *Lmna* 5' upstream sequences, 232 bp of 5' UTR sequences, and 244 bp of coding sequences in *Lmna* exon 1) (Supplementary Table S9).

Western blotting

Cell extracts from MEFs and SMCs were size-fractionated on 4–12% gradient SDS-polyacrylamide gels (Invitrogen), and the

separated proteins were transferred to nitrocellulose for western blots [10,11]. The membranes were blocked with Odyssey Blocking solution (LI-COR Biosciences) and then incubated overnight at 4°C with primary antibodies against the N terminus (exon 1) of lamin A/C and actin (both from Santa Cruz Biotechnology) (Supplementary Table S1). The membranes were then washed with PBS containing 0.3% Tween-20 and incubated with infrared dye (IR)-labeled secondary antibodies (Thermo Fisher) for 1 h at RT. Antibody binding was quantified with an Odyssey infrared scanner (LI-COR Biosciences).

Immunofluorescence microscopy

MEFs and SMCs were seeded onto µ-Slide 4-Well Glass Bottom plates (ibidi), fixed with 4% paraformaldehyde (PFA), and permeabilized with 0.2% Triton X-100 [11]. The cells were incubated with antibodies against lamin A/C (Santa Cruz Biotechnology), lamin B1 (Santa Cruz Biotechnology), and Lap2β (Invitrogen) (Supplementary Table S1), followed by Alexa Fluor – labeled secondary antibodies (Thermo Fisher, 1:1000) and DAPI (Thermo Fisher). Confocal images were acquired with an LSM980 microscope (Zeiss), a 63× objective, and 5–6× digital zoom. Identical imaging settings were maintained across all experiments; images were processed with Zen Blue software (Zeiss).

RT-PCR

RNA was extracted from *Lmna*^{+/+} and *Lmna*^{-/-} MEFs with the RNeasy Mini Kit (Qiagen). RNA quality and quantity were assessed with a NanoDrop 1000 Spectrophotometer (Thermo Scientific). A SMARTer RACE 5'/3' Kit (Takara Bio) employing a 3' oligo dT/adaptor sequence primer was used to generate 3'-RACE cDNA. To characterize *Lmna* transcripts from *Lmna*^{-/-} MEFs, the cDNA was used as a template for PCR reactions with a *Lmna* 5' UTR forward primer and a 3' reverse primer that binds to the adaptor sequence. Two 3'-RACE PCR products were detected in *Lmna*^{-/-} MEFs ("Transcript 1" and "Transcript 2"); the two amplicons were purified from 1% agarose gels with NucleoSpin Gel and

PCR Clean-up Kit (Macherey-Nagel) and sequenced directly (with primers listed in Supplementary Table S3). To analyze Transcript 2 in greater detail, nested PCR reactions were performed with primers F1 and R2 (exon 1–intron 7), primers F1 and R1 (exon 1–exon 12), and primers F2 and Short Universal Primer (exon 12 to the 3' adaptor). The exon 1–exon 12 and exon 12–adaptor amplicons were sequenced.

Cell transduction studies

Lmna^{-/-} SMCs were transduced with a lentiviral vector designed to express either of two truncated lamin A proteins: (i) a lamin A containing *Lmna* exon 1–7 sequences + 12 bp of intron 7 (encoding Val, Gly, Leu, followed by a stop codon) or (ii) a lamin A containing *Lmna* exon 1–7 + exon 12 sequences. To create the lentiviral vectors, the Dox-inducible pTRIPZ (Horizon) plasmid was digested with *Age*I and *Eco*RI and gel-purified [11]. The cDNAs for *Lmna* exon 1–7 + 12 bp of intron 7 and a cDNA for *Lmna* exon 1–7 + exon 12 were amplified from *Lmna*^{-/-} MEFs with the CloneAMP HiFi PCR Kit (Takara Bio) with forward primer 5'-

GTCAGATCGCACC GGCCACCATGGAGAC-CCCGTC-3' and either reverse primer 5'-GTAGCCCCTTGAATTTACAGGCCACCTC-G-3' (for Transcript 2–1) or reverse primer 5'-GTAGCCCCTTGAATTTTACATGATGCTGCA-GTTCTGGG-3' (for Transcript 2–2). Two different *Lmna* cDNAs were purified and introduced into the pTRIPZ vector with the In-Fusion

Cloning Kit (Takara Bio). The integrity of each plasmid was documented by DNA sequencing. Lentivirus packaging and cell transductions were performed by the UCLA Vector Core. The transduced cells were subjected to selection for 14 days in a medium containing puromycin (1.5 µg/mL). To induce *Lmna* expression, the cells were treated with 100 ng/mL doxycycline for 48 h.

Studies with a protein farnesyltransferase inhibitor (FTI)

Lmna^{+/+} MEFs and *Lmna*^{-/-} SMCs expressing the 'exon 1–7 + exon 12 truncated lamin A' were incubated in medium containing 1 µM tipifarnib (Sigma-Aldrich) for 48 h (for western blots) or 96 h (for immunocytochemistry studies).

Results

We confirmed, with western blots, the synthesis of a 54-kDa truncated lamin A in *Lmna*^{-/-} MEFs (Figure 1a). The intensity of the truncated lamin A band, normalized to the bands for either actin or lamin B1, was ~10% of the combined intensity of the lamin A and lamin C bands in *Lmna*^{+/+} MEFs (Figure 1b).

In *Lmna*^{+/+} MEFs, lamins A/C and lamin B1 (a farnesylated protein) are targeted to the nuclear rim, as judged by immunocytochemistry studies (Figure 2a). In *Zmpste24*^{-/-} MEFs, farnesyl – pre-lamin A was also located at the nuclear rim (Figure 2a). In *Lmna*^{-/-} MEFs, lamin B1 was targeted to the nuclear rim, but the truncated lamin

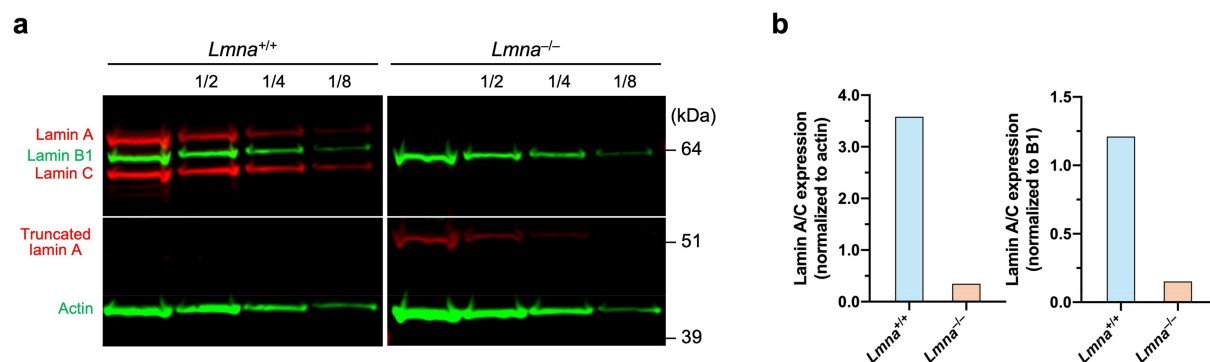


Figure 1. A 54-kDa truncated lamin a in *Lmna*^{-/-} MEFs. (a) Western blots (with lamin A/C – and lamin B1-specific antibodies) of serial dilutions of the concentrated lysates from *Lmna*^{+/+} and *Lmna*^{-/-} MEFs. A 54-kDa truncated lamin A was detected in *Lmna*^{-/-} MEFs. (b) The intensity of the truncated lamin A in *Lmna*^{-/-} MEFs, relative to actin or lamin B1, was only ~10% of the intensity of the total amount of lamin A and lamin C bands in *Lmna*^{+/+} MEFs (as judged by an infrared scanner).

A was predominantly nucleoplasmic (with only small amounts at the nuclear rim) (Figure 2b). In *Lmna*^{-/-}*Lmnb1*^{-/-}*Lmnb2*^{-/-} MEFs [6], the truncated lamin A was entirely nucleoplasmic (without any detectable enrichment along the nuclear rim) (Figure 2c).

The targeting of the truncated lamin A to the nucleoplasm in *Lmna*^{-/-} and *Lmna*^{-/-}*Lmnb1*^{-/-}*Lmnb2*^{-/-} MEFs, along with earlier studies showing nonfarnesylated prelamin A and nonfarnesylated lamin B1 in the nucleoplasm [12,13], prompted us to consider the possibility that the truncated lamin A in *Lmna*^{-/-} MEFs was not farnesylated – or that only very small amounts of the protein were farnesylated. To explore this issue, we began by characterizing *Lmna* transcripts in *Lmna*^{-/-} and *Lmna*^{+/+} MEFs. We prepared cDNAs from MEFs with a 3'-RACE kit employing an oligo dT primer with an adaptor sequence. Then, using a *Lmna*-specific 5' UTR primer and an adaptor sequence primer, we amplified *Lmna* transcripts. In *Lmna*^{+/+} MEFs, we identified prominent ~3-kb

and ~2.1-kb bands (consistent with transcripts for prelamin A and lamin C). In *Lmna*^{-/-} MEFs, we observed a strong ~4.7-kb band (Transcript 1) and a less intense ~1.9-kb band (Transcript 2) (Figure 3a).

Direct sequencing of Transcript 1 revealed *Lmna* exon 1–7 sequences, 131 bp of intron 7, the *Pgkneo* cassette in the reverse orientation, 162 bp from the 3' end of exon 11, followed by intron 11 and exon 12 sequences and the poly(A) tail (Supplementary Table S5). Transcript 1 encodes a 463-residue lamin A (460 amino acids from exon 1–7 followed by three amino acids encoded by intron 7 sequences).

Direct sequencing of Transcript 2 yielded unambiguous chromatograms revealing exon 1–7 sequences, 131 bp from intron 7, 158 bp from the *Pgkneo* cassette, followed by a poly(A) tail (Supplementary Table S6 and S7). These sequences encode the very same 463-residue lamin A encoded by Transcript 1. (By direct sequencing of Transcript 2, exon 12 sequences were not detected.)

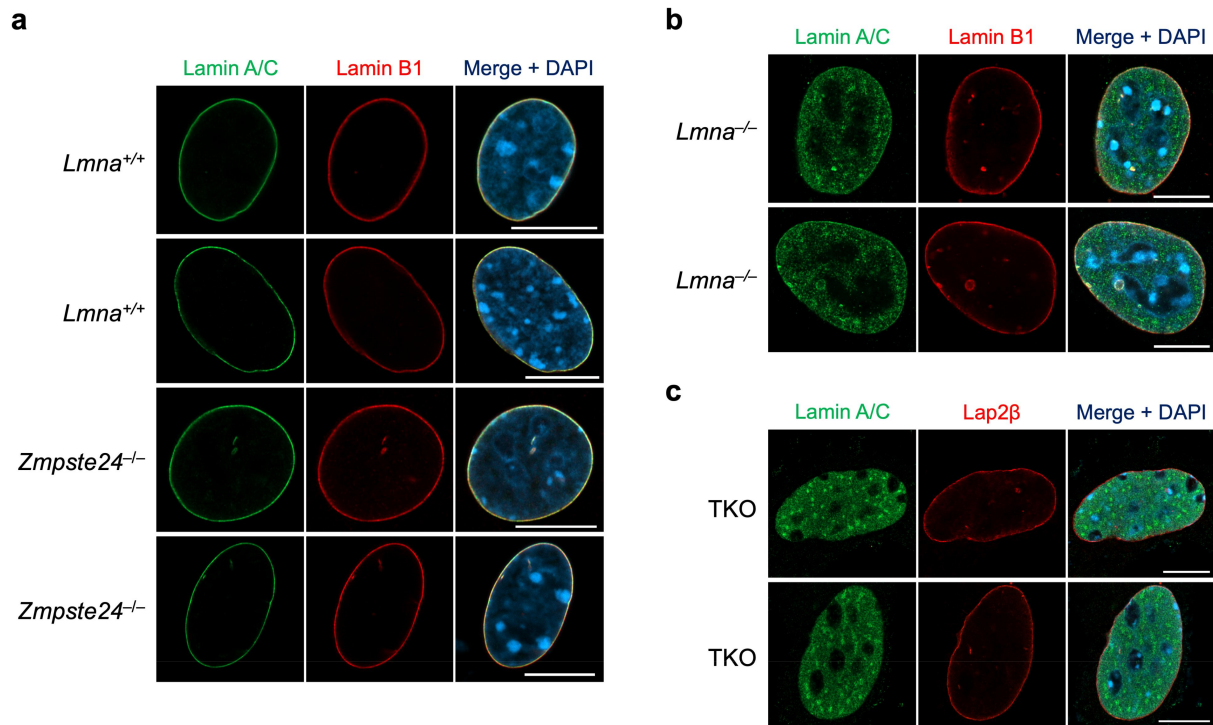


Figure 2. Nuclear lamin distribution in mouse embryonic fibroblasts (MEFs), as judged by immunofluorescence microscopy. Fixed and permeabilized MEFs were stained with lamin A/C- and lamin B1-specific antibodies, and confocal images across the middle of the nucleus (in the z-plane) were recorded. In *Lmna*^{+/+} and *Zmpste24*^{-/-} MEFs (a), the nuclear lamins were located along the nuclear rim. In *Lmna*^{-/-} MEFs (b), the truncated lamin A was predominantly nucleoplasmic but with detectable enrichment along the nuclear rim. In *Lmna*^{-/-}*Lmnb1*^{-/-}*Lmnb2*^{-/-} (TKO) MEFs (c), the truncated lamin A was entirely nucleoplasmic. Scale bars, 10 μ m.

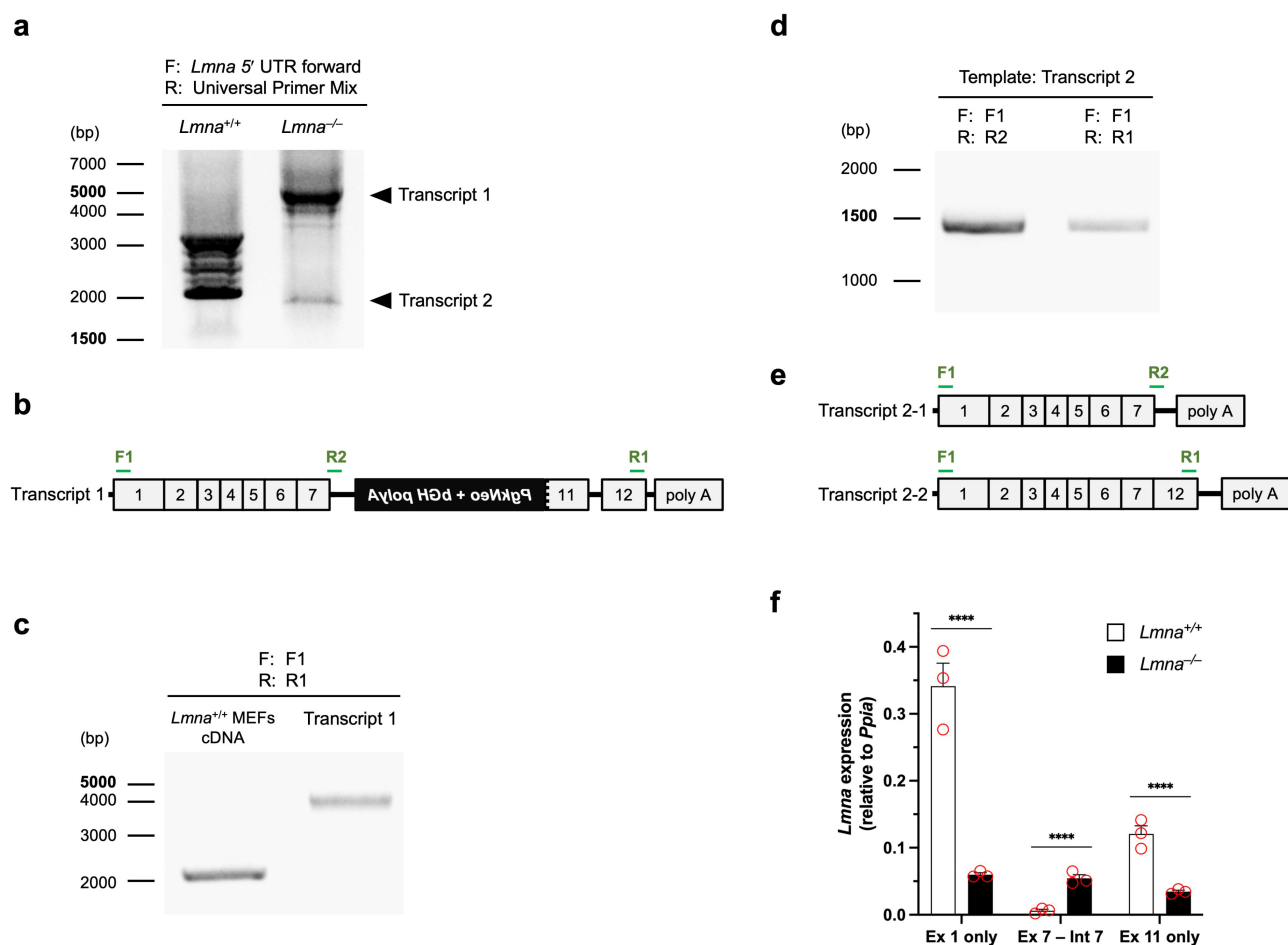


Figure 3. Analyzing *Lmna* transcripts in *Lmna*^{-/-} MEFs. (a) *Lmna* transcripts in *Lmna*^{+/+} and *Lmna*^{-/-} MEFs (defined by 3'-RACE PCR). *Lmna*^{-/-} MEFs had ~4.7-kb and ~1.9-kb transcripts (Transcript 1 and Transcript 2, respectively), whereas *Lmna*^{+/+} MEFs had strong ~3-kb and ~2.1-kb transcripts (for prelamin A and lamin C, respectively). (b) Transcript 1, defined by direct DNA sequencing, encoded a 463-residue lamin A (460 residues from exon 1–7 and three residues from intron 7 sequences). The location of F1, R1, and R2 are shown. Exons are not drawn to scale. (c) Nested PCR studies, using primers F1 (exon 1) and R1 (exon 12), on cDNA from *Lmna*^{+/+} MEFs and Transcript 1 from *Lmna*^{-/-} MEFs. These studies confirmed the existence of the very long *Lmna* transcript in *Lmna*^{-/-} MEFs. (d) Nested PCR studies on Transcript 2 from *Lmna*^{-/-} MEFs, using primer F1 (exon 1) and either primer R2 (intron 7) or R1 (exon 12). These studies revealed that Transcript 2 is a mixture of two transcripts: transcript 2–1 (containing exon 1–7 sequences) and Transcript 2–2 (containing exon 1–7 + exon 12 sequences). (e) Schematic of transcripts 2–1 and 2–2, as defined by DNA sequencing. Transcript 2–1 encodes the same 463-residue protein encoded by Transcript 1; Transcript 2–2 encodes a 468-residue protein (465 residues after posttranslational processing). (f) Quantitative RT-PCR studies to assess amounts of *Lmna* expression, relative to *Ppia*, in *Lmna*^{+/+} (white bars) and *Lmna*^{-/-} MEFs (black bars) (mean ± SEM, red circles depict three independent experiments). *Lmna* transcripts were more abundant in *Lmna*^{+/+} MEFs than in *Lmna*^{-/-} MEFs, as judged by a primer pair within exon 1. Transcripts containing intron 7 sequences were abundant in *Lmna*^{-/-} MEFs (*i.e.*, Transcript 1, Transcript 2–1) but were barely detectable in *Lmna*^{+/+} MEFs, as judged by an exon 7–intron 7 primer pair. Transcripts containing exon 11 sequences were present in *Lmna*^{-/-} MEFs (*i.e.*, Transcript 1) and in *Lmna*^{+/+} MEFs, as judged by a primer pair in the 3' portion of exon 11. *Lmna* transcript levels were compared by 2-way ANOVA (*****p* < 0.0001).

The absence of exon 12 sequences in Transcript 2 prompted us to gel-purify the Transcript 2 cDNA and perform nested PCR reactions with primers F1 and R2 (exon 1–intron 7) and primers F1 and R1 (exon 1–exon 12). Both PCR reactions yielded ~1.4-kb amplicons, implying that ‘Transcript 2’ is a mixture of two transcripts (‘Transcript 2–1’ and ‘Transcript 2–2’). The DNA

sequence of Transcript 2–1 (from the exon 1–intron 7 primer pair) was identical to sequence of the original Transcript 2 (which had been determined by direct sequencing of the ~1.9-kb 3'-RACE PCR product) (Supplementary Table S7). Transcript 2–2 (from the exon 1–exon 12 primer pair) contained exon 1–7 + exon 12 sequences and encodes a 468-residue lamin A (465 residues after

completion of posttranslational processing) (Supplementary Table S8). The existence of Transcript 2–2 explains the ability of Jahn *et al.* [2] to amplify a cDNA fragment containing 1–7 + exon 12 sequences.

Quantitative PCR studies revealed that *Lmna* expression was six-fold higher in *Lmna*^{+/+} MEFs than in *Lmna*^{-/-} MEFs, as judged by a primer pair within exon 1 (Figure 3f). Also, the expression of the 3' portion of exon 11 (present in the *Lmna* transcripts of *Lmna*^{+/+} MEFs and in Transcript 1 of *Lmna*^{-/-} MEFs) was ~3.5-fold higher in *Lmna*^{+/+} MEFs than in *Lmna*^{-/-} MEFs (Figure 3f). Transcripts containing intron 7 sequences (found in Transcript 1 and Transcript 2–1 of *Lmna*^{-/-} MEFs) were far more abundant in *Lmna*^{-/-} MEFs than in *Lmna*^{+/+} MEFs, as judged by PCR with an exon 7–intron 7 primer pair (Figure 3f).

We generated lentiviral expression vectors for a truncated lamin A containing exon 1–7 sequences + the three residues from intron 7 (corresponding to products of Transcript 1 and Transcript 2–1) and the truncated lamin A containing exon 1–7 + exon 12 sequences

(corresponding to the product of Transcript 2–2). When the two vectors were introduced into *Lmna*^{-/-} SMCs, both yielded a 54-kDa lamin A (Figure 4a). By immunocytochemistry, the 'exon 1–7 lamin A' was predominantly nucleoplasmic (with minimal enrichment along the nuclear rim), resembling the truncated lamin A in *Lmna*^{-/-} MEFs. In contrast, the 'exon 1–7 + exon 12 lamin A' was located at the nuclear rim, colocalizing with lamin B1. Thus, the presence of exon 12 (which encodes the *CaaX* motif that triggers protein farnesylation) results in the targeting of the truncated lamin A to the nuclear rim. We incubated *Lmna*^{+/+} MEFs as well as the *Lmna*^{-/-} SMCs expressing the 'exon 1–7 + exon 12 lamin A' with a protein farnesyltransferase inhibitor (FTI). In FTI-treated *Lmna*^{+/+} MEFs, nonfarnesylated prelamin A was documented by western blot and detected in the nucleoplasm by immunocytochemistry (Figure 5). In untreated *Lmna*^{+/+} MEFs, lamin A/C was found along the nuclear rim. In *Lmna*^{-/-} SMCs expressing the exon 1–7 + exon 12 lamin A, the FTI resulted in increased amounts of the lamin A in the nucleoplasm (Figure 5a).

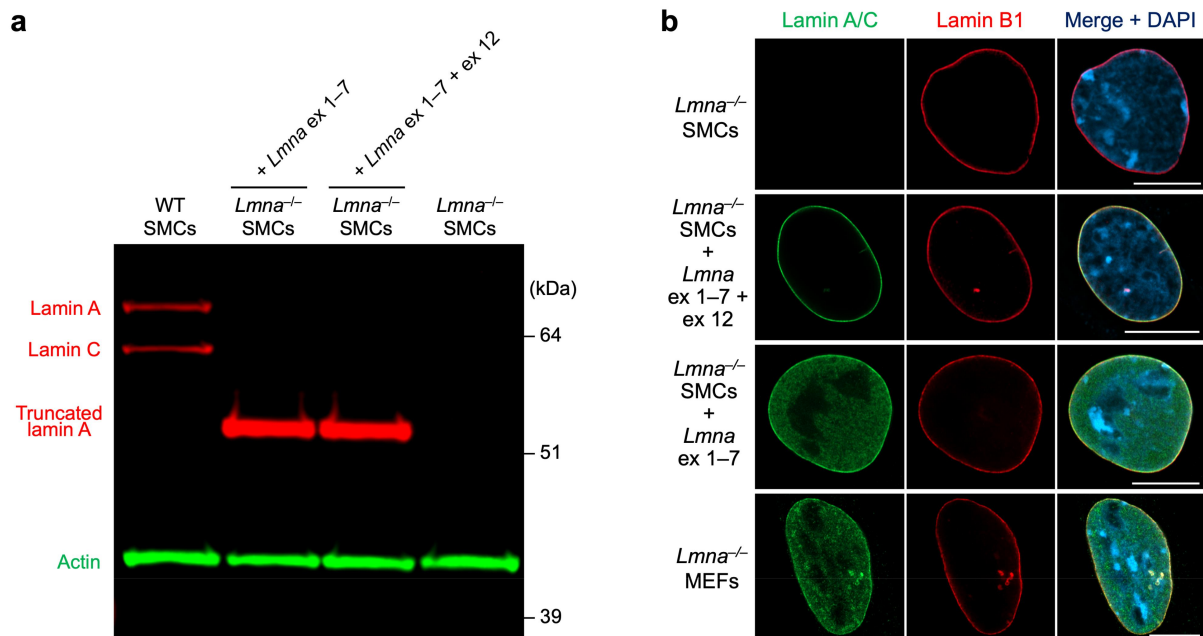


Figure 4. Expression of 54-kDa truncated lamin A proteins in *Lmna*^{-/-} smooth muscle cells (SMCs). A mutant lamin A containing exon 1–7 sequences (corresponding to Transcript 2–1) and a mutant lamin A containing exon 1–7 + exon 12 sequences (corresponding to Transcript 2–2) were expressed in *Lmna*^{-/-} SMCs. (a) Western blot of SMC extracts with lamin A/C – and actin-specific antibodies. (b) Confocal immunofluorescence micrographs across the middle of the cell nucleus in the z plane, revealing that the 'exon 1–7 lamin A' in *Lmna*^{-/-} SMCs was predominantly nucleoplasmic (resembling the distribution of the truncated lamin A in *Lmna*^{-/-} MEFs), whereas lamin B1 was located at the nuclear rim. In contrast, the 'exon 1–7 + exon 12 lamin A' was located along the nuclear rim in *Lmna*^{-/-} SMCs. Scale bars, 10 μ m.

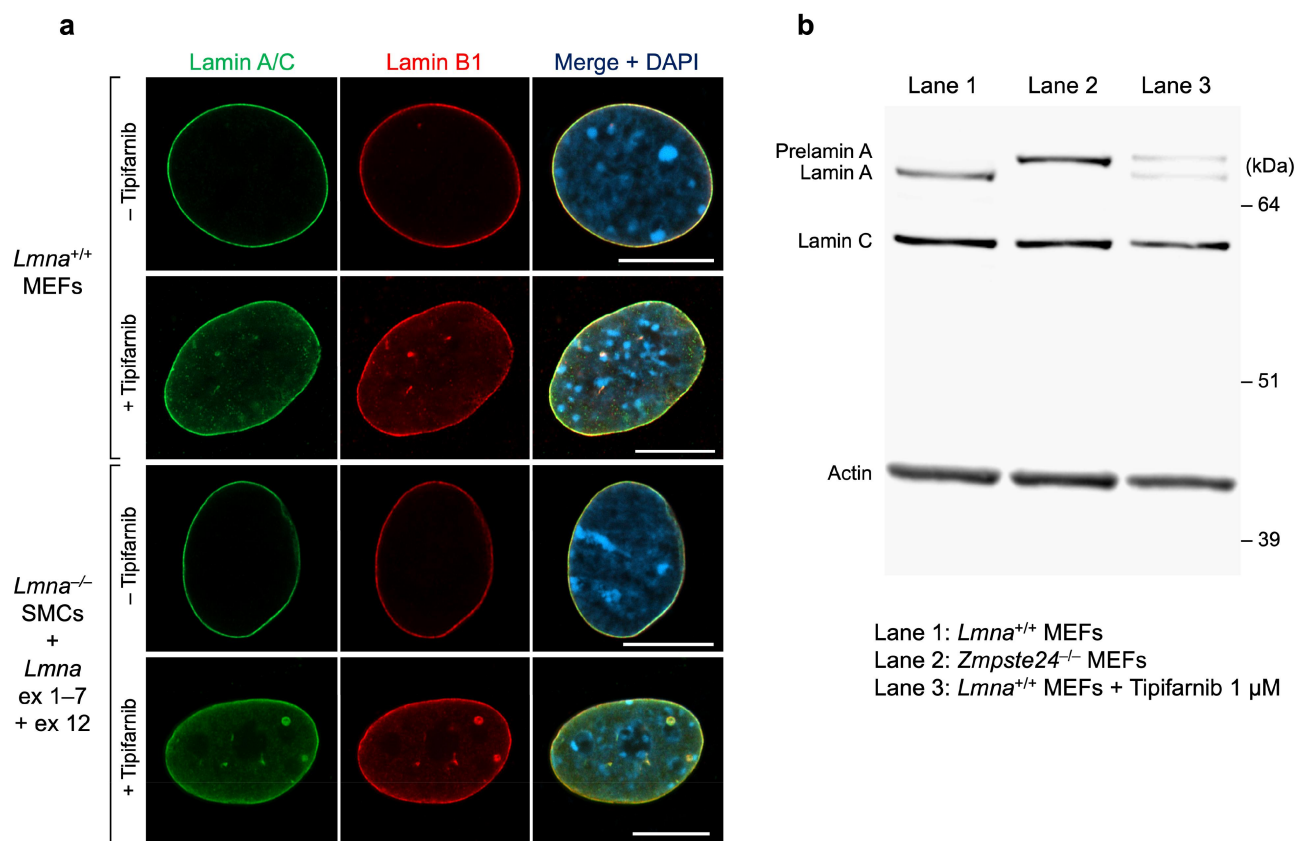


Figure 5. Nuclear lamin distribution in mouse embryonic fibroblasts (MEFs) that had been cultured in the presence of a protein farnesyltransferase inhibitor (FTI). (a) Confocal micrographs of *Lmna*^{+/+} MEFs and *Lmna*^{-/-} SMCs that expressed the exon 1–7 + exon 12 lamin A (cultured in the presence or absence of 1 μ M tipifarnib). Scale bars, 10 μ m. (b) A western blot, with antibodies against lamin A/C and actin, of cell extracts from *Lmna*^{+/+} MEFs, *Zmpste24*^{-/-} MEFs, and *Lmna*^{+/+} MEFs that had been incubated with 1 μ M tipifarnib.

Discussion

The *Lmna*^{-/-} mice created by Sullivan *et al.* [1] were important because they revealed that lamin A/C deficiency causes a cardiomyopathy and a lethal muscular dystrophy and misshapen nuclei in MEFs. Over the past two decades, the Sullivan *Lmna*^{-/-} mice have been used in numerous studies of lamin A function [3–7,14–17]. The Sullivan *Lmna* knockout allele was initially reported to be a null allele [1], but Jahn *et al.* [2] discovered that it produces a 54-kDa truncated lamin A. The transcripts from the *Lmna* knockout allele that accounted for the truncated lamin A were not characterized, but Jahn *et al.* [2] were able to detect, by RT-PCR, a *Lmna* cDNA amplicon containing exon 1–7 + exon 12 sequences. Because exon 12 encodes prelamins A's CaaX motif, the truncated lamin A was assumed to be farnesylated.

In the current studies, we revisited the Sullivan knockout allele because we were puzzled by the fact that the truncated lamin A in *Lmna*^{-/-} MEFs was largely nucleoplasmic, whereas lamin B1 was located at the nuclear rim. Lamins A/C and lamin B1 in *Lmna*^{+/+} MEFs – and farnesyl – prelamins A in *Zmpste24*^{-/-} MEFs – were located at the nuclear rim.

The nucleoplasmic location of the truncated lamin A in *Lmna*^{-/-} MEFs prompted us to consider the possibility that it was not farnesylated. To examine this possibility, we analyzed *Lmna* transcripts in *Lmna*^{-/-} MEFs. By 3'–RACE PCR, we identified ~4.7-kb and ~1.9-kb transcripts. The ~4.7-kb transcript produces a 463–amino acid lamin A containing residues encoded by exon 1–7 sequences + three residues encoded by intron 7. The ~1.9-kb amplicon proved to be a mixture of two transcripts – an abundant transcript (Transcript 2–1, which contains exon 1–7

sequences and encodes the very same 463-residue lamin A) and a small amount of another transcript (Transcript 2–2, which contains exon 1–7 + exon 12 sequences and encodes a 468-residue lamin A with a C-terminal *CaaX* motif). Thus, Transcript 1 and Transcript 2–1 were the main transcripts; both encode a 463-residue exon 1–7 lamin A. Transcript 2–2 (which contains exon 12 sequences) was present in very low amounts. Consistent with that conclusion, direct sequencing of Transcript 2 yielded unambiguous chromatographs and failed to uncover doublet peaks (Supplementary Table S6).

Our study provided quantitative insights into amounts of lamin A transcripts and proteins in *Lmna*^{-/-} MEFs. The level of exon 1-containing transcripts in *Lmna*^{-/-} MEFs was only ~18% of the level in *Lmna*^{+/+} MEFs, as judged by quantitative RT-PCR. By western blot, the amount of truncated lamin A in *Lmna*^{-/-} MEFs (normalized to either actin or lamin B1) was only ~10% of the total amount of lamin A and lamin C in *Lmna*^{+/+} MEFs.

We predicted that the ‘exon 1–7 lamin A’ would be targeted to the nucleoplasm, whereas the ‘exon 1–7 + exon 12 lamin A’ would be targeted to the nuclear rim. Indeed, that was the case; our cell transduction studies revealed that the ‘exon 1–7 lamin A’ was predominantly nucleoplasmic, whereas the ‘exon 1–7 + exon 12 lamin A’ was targeted to the nuclear rim.

While the truncated lamin A in *Lmna*^{-/-} MEFs was predominantly nucleoplasmic, some enrichment of the protein could be detected along the nuclear rim. In *Lmna*^{-/-}*Lmnb1*^{-/-}*Lmnb2*^{-/-} MEFs, the truncated lamin A was entirely nucleoplasmic (absent nuclear rim enrichment). Thus, in the *Lmna*^{-/-} MEFs, we suspect that the small amounts of the truncated lamin A along the nuclear rim resulted from interactions between the truncated lamin A and the B-type nuclear lamins.

One could argue that our experimental findings were foreshadowed by results in the Sullivan *et al.* [1] and Jahn *et al.* [2] publications. First, the northern blot by Sullivan *et al.* [1] revealed two different *Lmna* transcripts in *Lmna*^{-/-} MEFs but those mRNAs were not characterized. It is conceivable that the bands observed in the northern blot corresponded to the transcripts that we uncovered by 3'-RACE and DNA sequencing. Second, proteomics studies by Jahn *et al.* [2] on the

truncated lamin A in *Lmna*^{-/-} MEFs uncovered exon 1–7 peptides but failed to uncover peptides from exon 12. They attributed the failure to find exon 12 peptides to the hydrophobicity of a farnesylated peptide. We agree that this explanation is plausible, but our studies suggest that the most likely explanation is that the vast majority of the 54-kDa truncated lamin A in *Lmna*^{-/-} MEFs lacks exon 12 sequences.

The Sullivan *Lmna*^{-/-} mice [1], which produce a truncated lamin A, have been widely used to study lamin A/C function [3–7,14–17]. It is noteworthy that the Sullivan *Lmna*^{-/-} mice succumb to cardiomyopathy/muscular dystrophy at 6–8 weeks of age. Another line of *Lmna*^{-/-} mice containing a gene-trap insertion in intron 1 survived for 2–3 weeks [18]. In those mice, lamin A was not detected in MEFs by western blot or immunocytochemistry. A third line of *Lmna*^{-/-} mice with a deletion spanning from intron 9 to the 3' UTR of exon 12 [19] did not appear to produce lamin A/C (as judged by immunostaining) and died ~2.5 weeks after birth. It is possible that the synthesis of truncated lamin A in the Sullivan *Lmna*^{-/-} mice led to longer postnatal survival.

The *Lmna*^{-/-} knockout mice created by Sullivan *et al.* [1] have been widely used to study lamin A/C [3–7,14–17], and they continue to be distributed by The Jackson Laboratory. In our opinion, the Sullivan *Lmna* knockout mice remain useful for some experimental purposes, but the potential impact of truncated lamin A will always need to be considered. Our studies are important because they add to our understanding of truncated lamin A from the Sullivan *Lmna* knockout allele.

Acknowledgments

Virus production and transduction were performed by the IMTC/UCLA Vector Core, which is supported by CURE/P30 DK041301. Flow cytometry was performed in the UCLA Jonsson Comprehensive Cancer Center (JCCC) and Center for AIDS Research Flow Cytometry Core Facility that is supported by the National Institutes of Health awards P30 CA016042 and 5P30 AI028697, and by the JCCC, the UCLA AIDS Institute, the David Geffen School of Medicine at UCLA, the UCLA Chancellor's Office, and the UCLA Vice Chancellor's Office of Research.

Disclosure statement

No potential conflict of interest was reported by the author(s).

Funding

The author(s) reported that there is no funding associated with the work featured in this article.

Data availability statement

The data supporting the findings of this study are available within the article and its supplementary materials from Supplementary file 1 and Supplementary file 2.

Author contributions

J.R.K. and S.G.Y. designed research; J.R.K., P.H.K., A.S., and Y.T. performed research; J.R.K. and S.G.Y. analyzed data; and J.R.K. and S.G.Y. wrote the paper.

ORCID

Joonyoung R. Kim  <http://orcid.org/0009-0009-1276-6971>

Paul H. Kim  <http://orcid.org/0000-0002-8429-651X>

Yiping Tu  <http://orcid.org/0000-0002-4630-9113>

Stephen G. Young  <http://orcid.org/0000-0001-7270-3176>

References

- [1] Sullivan T, Escalante-Alcalde D, Bhatt H, et al. Loss of A-type lamin expression compromises nuclear envelope integrity leading to muscular dystrophy. *J Cell Bio.* 1999;147(5):913–919. doi: [10.1083/jcb.147.5.913](https://doi.org/10.1083/jcb.147.5.913)
- [2] Jahn D, Schramm S, Schnolzer M, et al. A truncated lamin A in the *Lmna* $-/-$ mouse line: implications for the understanding of laminopathies. *Nucleus.* 2012;3(5):463–474. doi: [10.4161/nucl.21676](https://doi.org/10.4161/nucl.21676)
- [3] Fong LG, Ng JK, Meta M, et al. Heterozygosity for *Lmna* deficiency eliminates the progeria-like phenotypes in *Zmpste24*-deficient mice. *Proc Natl Acad Sci U S A.* 2004;101(52):18111–18116. doi: [10.1073/pnas.0408558102](https://doi.org/10.1073/pnas.0408558102)
- [4] Lammerding J, Fong LG, Ji JY, et al. Lamins a and C but not lamin B1 regulate nuclear mechanics. *J Biol Chem.* 2006;281(35):25768–25780. doi: [10.1074/jbc.M513511200](https://doi.org/10.1074/jbc.M513511200)
- [5] Jung HJ, Tatar A, Tu Y, et al. An absence of nuclear lamins in keratinocytes leads to ichthyosis, defective epidermal barrier function, and intrusion of nuclear membranes and endoplasmic reticulum into the nuclear chromatin. *Mol Cell Biol.* 2014;34(24):4534–4544. doi: [10.1128/MCB.00997-14](https://doi.org/10.1128/MCB.00997-14)
- [6] Chen NY, Kim P, Weston TA, et al. Fibroblasts lacking nuclear lamins do not have nuclear blebs or protrusions but nevertheless have frequent nuclear membrane ruptures. *Proc Natl Acad Sci U S A.* 2018;115(40):10100–10105. doi: [10.1073/pnas.1812622115](https://doi.org/10.1073/pnas.1812622115)
- [7] Chen NY, Kim PH, Tu Y, et al. Increased expression of LAP2 β eliminates nuclear membrane ruptures in nuclear lamin-deficient neurons and fibroblasts. *Proc Natl Acad Sci U S A.* 2021;118(25). doi: [10.1073/pnas.2107770118](https://doi.org/10.1073/pnas.2107770118)
- [8] Yang SH, Bergo MO, Toth JI, et al. Blocking protein farnesyltransferase improves nuclear blebbing in mouse fibroblasts with a targeted Hutchinson-Gilford progeria syndrome mutation. *Proc Natl Acad Sci U S A.* 2005;102(29):10291–10296. doi: [10.1073/pnas.0504641102](https://doi.org/10.1073/pnas.0504641102)
- [9] Kim PH, Luu J, Heizer P, et al. Disrupting the LINC complex in smooth muscle cells reduces aortic disease in a mouse model of Hutchinson-Gilford progeria syndrome. *Sci Transl Med.* 2018;10(460). doi: [10.1126/scitranslmed.aat7163](https://doi.org/10.1126/scitranslmed.aat7163)
- [10] Heizer PJ, Yang Y, Tu Y, et al. Deficiency in ZMPSTE24 and resulting farnesyl–prelamin A accumulation only modestly affect mouse adipose tissue stores. *J Lipid Res.* 2020;61(3):413–421. doi: [10.1194/jlr.RA119000593](https://doi.org/10.1194/jlr.RA119000593)
- [11] Kim PH, Chen NY, Heizer PJ, et al. Nuclear membrane ruptures underlie the vascular pathology in a mouse model of Hutchinson-Gilford progeria syndrome. *JCI Insight.* 2021;6(16). doi: [10.1172/jci.insight.151515](https://doi.org/10.1172/jci.insight.151515)
- [12] Jung HJ, Nobumori C, Goulbourne CN, et al. Farnesylation of lamin B1 is important for retention of nuclear chromatin during neuronal migration. *Proc Natl Acad Sci U S A.* 2013;110(21):E1923–1932. doi: [10.1073/pnas.1303916110](https://doi.org/10.1073/pnas.1303916110)
- [13] Davies BS, Barnes RH 2nd, Tu Y, et al. An accumulation of non-farnesylated prelamin A causes cardiomyopathy but not progeria. *Hum Mol Genet.* 2010;19(13):2682–2694. doi: [10.1093/hmg/ddq158](https://doi.org/10.1093/hmg/ddq158)
- [14] Wolf CM, Wang L, Alcalai R, et al. Lamin A/C haploinsufficiency causes dilated cardiomyopathy and apoptosis-triggered cardiac conduction system disease. *J Mol Cell Cardiol.* 2008;44(2):293–303. doi: [10.1016/j.yjmcc.2007.11.008](https://doi.org/10.1016/j.yjmcc.2007.11.008)
- [15] Mehl JL, Earle A, Lammerding J, et al. Blockage of lamin-A/C loss diminishes the pro-inflammatory macrophage response. *iScience.* 2022;25(12):105528. doi: [10.1016/j.isci.2022.105528](https://doi.org/10.1016/j.isci.2022.105528)
- [16] Brayson D, Shanahan CM. Lamin A precursor localizes to the Z-disc of sarcomeres in the heart and is dynamically regulated in muscle cell differentiation. *Philos Trans R Soc Lond B Biol Sci.* 2022;377(1864):20210490. doi: [10.1098/rstb.2021.0490](https://doi.org/10.1098/rstb.2021.0490)
- [17] Earle AJ, Kirby TJ, Fedorchak GR, et al. Mutant lamins cause nuclear envelope rupture and DNA damage in skeletal muscle cells. *Nat Mater.* 2020;19(4):464–473. doi: [10.1038/s41563-019-0563-5](https://doi.org/10.1038/s41563-019-0563-5)
- [18] Kubben N, Voncken JW, Konings G, et al. Post-natal myogenic and adipogenic developmental: defects and metabolic impairment upon loss of A-type lamins. *Nucleus.* 2011;2(3):195–207. doi: [10.4161/nucl.2.3.15731](https://doi.org/10.4161/nucl.2.3.15731)
- [19] Solovei I, Wang AS, Thanisch K, et al. LBR and lamin A/C sequentially tether peripheral heterochromatin and inversely regulate differentiation. *Cell.* 2013;152(3):584–598. doi: [10.1016/j.cell.2013.01.009](https://doi.org/10.1016/j.cell.2013.01.009)